Arch Toxicol
DOI 10.1007/s00204-013-1096-3

IN VITRO SYSTEMS

Effects of *N*-acetyl-L-cysteine on target sites of hydroxylated fullerene-induced cytotoxicity in isolated rat hepatocytes

Yoshio Nakagawa · Toshinari Suzuki · Kazuo Nakajima · Akiko Inomata · Akio Ogata · Dai Nakae

Received: 14 May 2013 / Accepted: 11 July 2013

Abstract The effects of *N*-acetyl-L-cysteine (NAC) on cytotoxicity caused by a hydroxylated fullerene [$C_{60}(OH)_{24}$], which is known a nanomaterial and/or a water-soluble fullerene derivative, were studied in freshly isolated rat hepatocytes. The exposure of hepatocytes to $C_{60}(OH)_{24}$ at a concentration of 0.1 mM caused time (0–3 h)-dependent cell death accompanied by the formation of cell blebs, loss of cellular ATP, and reduced glutathione (GSH) and protein thiol levels, as well as the accumulation of glutathione disulfide and malondialdehyde (MDA), indicating lipid peroxidation. Despite this, $C_{60}(OH)_{24}$-induced cytotoxicity was effectively prevented by NAC pretreatment ranging in concentrations from 1 to 5 mM. Further, the loss of mitochondrial membrane potential (MMP) and generation of oxygen radical species in hepatocytes incubated with $C_{60}(OH)_{24}$ were inhibited by pretreatment with NAC, which caused increases in cellular and/or mitochondrial levels of GSH, accompanied by increased levels of cysteine via enzymatic deacetylation of NAC. On the other hand, severe depletion of cellular GSH levels caused by diethyl maleate at a concentration of 1.25 mM led to the enhancement of $C_{60}(OH)_{24}$-induced cell death accompanied by a rapid loss of ATP. Taken collectively, these results indicate that pretreatment with NAC ameliorates (a) mitochondrial dysfunction linked to the depletion of ATP, MMP, and mitochondrial GSH level and (b) induction of oxidative stress assessed by reactive oxygen species generation, losses of intracellular GSH and protein thiol levels, and MDA formation caused by $C_{60}(OH)_{24}$, suggesting that the onset of toxic effects is at least partially attributable to a thiol redox-state imbalance as well as mitochondrial dysfunction related to oxidative phosphorylation.

Keywords Hydroxylated fullerene · Fullerenol · Mitochondrial dysfunction · Oxidative stress · *N*-acetyl-L-cysteine · Cytotoxicity · Rat hepatocytes

Abbreviations

DEM	Diethyl maleate
DCHF-DA	2′,7′-Dichlorodihydrofluorescein diacetate
DNP-NAC	2,4-Dinitrophenyl *S*-conjugate of *N*-acetyl-L-cysteine
DMSO	Dimethyl sulfoxide
GSH	Glutathione
GSSG	Glutathione disulfide
HEPES	*N*-(2-hydroxyethyl)-piperazine-*N*-(2-ethanesulfonic acid)
MDA	Malondialdehyde
MPT	Mitochondrial permeability transition
NAC	*N*-acetyl-L-cysteine
ROS	Reactive oxygen species
MMP	Mitochondrial membrane potential

Y. Nakagawa (✉) · A. Inomata · A. Ogata · D. Nakae
Division of Toxicology, Tokyo Metropolitan Institute of Public Health, 3-24-1, Hyakunin-cho, Shinjuku-ku, Tokyo 169-0073, Japan
e-mail: Yoshio_1_Nakagawa@member.metro.tokyo.jp

T. Suzuki
Division of Environmental Health, Tokyo Metropolitan Institute of Public Health, 3-24-1, Hyakunin-cho, Shinjuku-ku, Tokyo 169-0073, Japan

K. Nakajima
Division of Food Additives, Tokyo Metropolitan Institute of Public Health, 3-24-1, Hyakunin-cho, Shinjuku-ku, Tokyo 169-0073, Japan

Published online: 23 July 2013

Author's personal copy

Introduction

Fullerenes, C_{60} and/or larger, are nanospheres as well as nanomaterials derived from carbon atoms and have been the focus of increasing interest for possible applications in multipronged industrial fields such as electronic engineering, pharmaceuticals, medical devices, cosmetics, and other boundary region industries since their discovery in 1985 (Kroto et al. 1985). While fullerene derivatives synthesized by the addition of reactive functional groups, such as hydroxyl-, carboxyl-, amino-, and alkyl-groups and other side-chain/cyclic moieties, to the C_{60} structure are widely produced in amounts of several tons per year (Borm et al. 2006), actual commercialization is still mostly under development. This trend is expected to result in the ever-increasing presence of nanomaterials in the human environment, although relatively little is known about the potential biological risks of nanomaterials, including fullerenes and their derivatives. Therefore, the relationship between these nanomaterials and their target sites in the body and/or tissues and cells has recently become an important theme of biological and/or toxicologic research.

Although fullerenes are generally hydrophobic molecules and are not water-soluble, chemical modification of the fullerene C_{60} molecule through the participation of hydrophilic addends such as hydroxyl groups leads to various polyhydroxylated fullerenes, also termed either fullerenols or fullerols, such as $C_{60}(OH)_n$, some of which show improved solubility in biological media. The enhancement of hydrophilicity was correlated with an increase in the number of hydroxyl groups in fullerenes, which induce their biological activities. Some fullerenols are potential candidates for pharmacological applications, including scavengers of oxygen radical species (Murugan et al. 2002; Tsai et al. 1997), protective agents against chemical-induced organ (Injac et al. 2008, 2009) and/or cell damages (Bogdanović et al. 2004), and neuroprotective and anticancer agents (Chen et al. 2005; Jin et al. 2000). Sayes et al. (2004) reported that in cell lines derived from human dermal fibroblasts, the cytotoxicity of water-soluble fullerenols [$C_{60}(OH)_n$] may be associated with specific functions of surface derivatization on C_{60}. On the other hand, fullerenols such as $C_{60}(OH)_{7\pm2}$ and $C_{60}(OH)_{24}$ caused cytotoxicity in RAW 264.7 cells (Chen et al. 2004) and in vascular endothelial cells (Yamawaki and Iwai 2006), respectively. Furthermore, fullerenols are thought to have cytotoxic/phototoxic (Isakovic et al. 2006; Roberts et al. 2008), genotoxic, and mutagenic effects in CHO, Hela, and HEK293 cell lines, respectively (Mrdanović et al. 2009; Niwa and Iwai 2007). Thus, the results from in vitro studies suggest that fullerenols exert cytotoxic as well as protective effects on various cell lines.

The liver is a major organ for the metabolism and detoxification of drugs and xenobiotics absorbed from the alimentary tract, and it may be highly susceptible to injury by these compounds at any time. When nanomaterials are inhaled through respiration, absorbed through the skin, or administered by intravenous injection, they enter the blood stream and are translocated to the liver (Sadauskas et al. 2007). Because blood containing these compounds passes through the liver before being distributed throughout the body, the liver is a potential target organ of nanomaterials. It was shown that some nanoparticles present in rat liver after intravenous administration induce oxidative stress locally after nanoparticle phagocytosis (Hoet et al. 2004). The freshly isolated rat hepatocyte system, which retains intact membranes and has high levels of various drug-metabolizing enzymes and their cofactors and multiple defense systems against intracellular oxidative stress produced by various chemicals as well as intact liver cells in the body, is useful for the study of the pharmacokinetics, intracellular target sites, morphologic/physiologic degeneration, and temporal sequences leading to cell injury induced by xenobiotics.

Although in vivo and in vitro studies confirmed that fullerenes and their derivatives could cross the external cellular membrane and accumulate in cells and/or tissues (Foley et al. 2002; Yamawaki and Iwai 2006), little is known of their cytotoxic effects and mechanisms of action on rat hepatocytes. Our previous study indicated that fullerenols such as $C_{60}(OH)_{24}$ and $C_{60}(OH)_{12}$ elicit cytotoxicity through mitochondrial failure related to the induction of the membrane permeability transition (MPT), mitochondrial depolarization, and inhibition of ATP synthesis, accompanied by rapid oxidation of cellular glutathione (GSH) and protein thiols (Nakagawa et al. 2011). It is well known that reduced GSH, a major cellular antioxidant and/or nucleophilic agent, is affected immediately by various forms of oxidative stress and xenobiotic detoxification in liver cells. In connection with this, *N*-acetyl-L-cysteine (NAC) is used as an effective acetylated precursor for reduced GSH in hepatocytes, and its application in different diseases including cancer, cardiovascular disorders, and chemical and metal toxicity has been reviewed previously (Zafarullah et al. 2003). In the present study, we investigated the protective effects of NAC against hydroxylated fullerene $C_{60}(OH)_{24}$-induced cytotoxicity in isolated rat hepatocytes. The mechanism of fullerene toxicity is also discussed.

Materials and methods

Materials

The chemical compounds used were obtained from the following companies: hydroxylated fullerene $C_{60}(OH)_{24}$ (fullerenol, purity of >99.5 %) from Materials Technologies

Research Ltd. (Cleveland, OH, USA), collagenase, NAC, L-cysteine and 1-fluoro-2,4-dinitrobenzene from Wako Pure Chemical Industries Ltd. (Osaka, Japan), glutathione (GSH), glutathione disulfide (GSSG), *N*-(2-hydroxyethyl)-piperazine-*N*-(2-ethanesulfonic acid) (HEPES), bovine serum albumin, diethyl maleate (DEM), 2′,7′-Dichlorodihydrofluorescein diacetate (DCHF-DA), and rhodamine 123 from Sigma Chemical Co. (St. Louis, MO, USA). All other chemicals were of the highest purity commercially available. Molecular formula of the fullerenol used in this study was assumed to be that reported by the manufacturer.

Isolation and cell culture incubation of hepatocytes

Male F344/Jcl (200–250 g) rats were obtained from CLEA Japan Inc. (Tokyo, Japan) and were housed in wire-bottom cages. The rats were allowed food (CE-2, CLEA Japan Inc., Tokyo) and water ad libitum. All animal husbandry and experimental procedures were approved under the Tokyo Metropolitan Institute of Public Health guidelines for the care and use of laboratory animals. After the rats were anesthetized with diethyl ether by inhalation, hepatocytes (1×10^6 cells/ml) were isolated by in situ two-step collagenase perfusion of the liver and suspended in Krebs–Henseleit buffer, pH 7.4, containing 12.5 mM HEPES and 0.1 % albumin, as described previously (Moldéus et al. 1978). All incubations were performed in rotating, round-bottomed flasks at 37 °C, under a constant flow of humidified carbogen (95 % O_2/5 % CO_2). The fullerenol $C_{60}(OH)_{24}$ was dissolved in dimethyl sulfoxide (DMSO) and sonicated for 30 min before the addition to hepatocyte suspensions. Reactions were initiated by addition of $C_{60}(OH)_{24}$ dissolved in DMSO (final concentration <0.5 %). In some experiments, prior to the addition of the fullerenol, the isolated hepatocytes were preincubated with NAC (final concentrations 1–5 mM) dissolved in Krebs–Henseleit buffer for 20 min or diethyl maleate (DEM, final concentration 1.25 mM) dissolved in DMSO for 15 min, respectively. The concentrations of NAC and DEM used here were obtained from previous studies (Nakagawa et al. 1993; Tirmenstein et al. 2000). Corresponding control groups received an equivalent volume of DMSO or Krebs–Henseleit buffer. Aliquots of incubation mixture were taken at intervals to monitor cell death and the concentrations of intracellular adenine nucleotides, GSH, GSSG, cysteine, reduced protein thiols, NAC, malondialdehyde (MDA), and reactive oxygen species (ROS).

Biochemical and morphological assays

Adenine nucleotides (ATP, ADP, and AMP) in hepatocytes were determined using a modified HPLC system, as described by Jones (1981). GSH, GSSG, and cysteine levels were determined by HPLC essentially as described by Reed et al. (1980). Reduced protein thiol concentrations were determined by using Ellman's reagent [5,5′-dithiobis-(2-nitrobenzoic acid)], as described previously (Albano et al. 1985). Protein was determined by the method of Lowry et al. (1951), using bovine serum albumin as the standard. MDA was measured as thiobarbituric acid-reactive products, as described previously (Sandy et al. 1986), and the amount of reactive product formed was calculated by using an extinction coefficient of 156 mM/cm. To assess hepatocyte viability, an equal volume of trypan blue solution (final concentration 0.08 %) was added into an aliquot of hepatocyte suspensions and the mixture was loaded into a hemacytometer. Cell viability was assayed by counting the number of cells excluding trypan blue in a Burker's chamber placed under a light microscope; at the same time, the number of blebbed hepatocytes excluding trypan blue-stained hepatocytes was also counted and was expressed as the percentage of viable hepatocytes exhibiting multiple surface protrusions (cell blebs). The initial cell viability in each experiment was more than 85 %.

Synthesis of 2,4-dinitrophenyl *S*-conjugate of NAC (DNP-NAC) and determination of its conjugate

The 2,4-dinitrophenyl *S*-conjugate of NAC was prepared as described by Hinchman et al. (1991), using 1-fluoro-2,4-dinitrobenzene as a derivatizing agent and was identified by LC–MS and ^{1}H-NMR. ^{1}H-NMR spectra were obtained with a model JNM-A500 spectrometer (JOEL Ltd, Tokyo, Japan) operated at 500 MHz. Tetradeuteromethanol (methanol-d_4) was used as a solvent, and all chemical shifts (ppm) were referenced to the intrinsic value for the solvent. The chemical shifts and assignments for ^{1}H were as follows: δ 1.98 (s, 3H), 3.43–3.76 (m, 2H), 4.72–4.75 (m, 1H), 7.92–8.07 (d, 1H), 8.45–8.47 (d, 1H), and 8.96–8.97 (d, 1H). The negative electrospray ionization (−ESI)/MS spectrum of DNP-NAC conjugate showed a peak at m/z 328, corresponding to $[M–H]^-$. After NAC in hepatocyte suspensions was reacted with 1-fluoro-2,4-dinitrobenzene, chemical shifts of its derivative obtained were corresponded to the data showed by Hinchman et al. (1991) and Pombrio et al. (2001).

Determination of mitochondrial membrane potential

Mitochondrial membrane potential (MMP) in hepatocytes was determined with rhodamine 123, a fluorescence probe which selectively enters mitochondria with an intact membrane potential and is retained in the mitochondria (Lemasters et al. 1993). Hepatocytes (1×10^6 cells/ml) were preincubated with NAC dissolved in Krebs–Henseleit buffer (final concentrations 1, 2.5, and 5 mM) for 20 min before the addition of fullerenol at a concentration of 0.1 mM. After 45 min, aliquots of cell suspensions were incubated with rhodamine 123 (1 μM) at 37 °C for 15 min. Following this incubation, hepatocytes pellets were obtained by the centrifugation at $100\times g$ for 5 min and were washed with Krebs–Henseleit buffer and then centrifuged again. The pellets obtained were resuspended in the same buffer containing 0.1 % Triton X-100. After 10 min, samples were centrifuged $1{,}600\times g$ for 5 min to remove any cellular debris. The concentration of rhodamine 123 in the supernatant medium was measured in a CytoFluor 4000 multiwell fluorescence plate reader (PerSeptive Biosystems Inc., Framingham, MA, USA): The extinction and emission filters were set at 485 nm (bandwidth ±10 nm) and 530 nm (bandwidth ±12.5 nm), respectively. The results are expressed as percentages of the fluorescence values for the untreated hepatocytes.

Author's personal copy

Detection of reactive oxygen species produced by fullerenol

A fluorescence-based microplate assay as described by Wang and Joseph (1999) was used for the evaluation of ROS in hepatocytes treated with $C_{60}(OH)_{24}$. The formation of intracellular ROS was measured by DCHF-DA. Viable cells deacetylate DCHF-DA to DCHF, which is not fluorescent, but reacts quantitatively with ROS (H_2O_2 and O_2^-) in cells to form fluorescent dye. Hepatocytes (1×10^6 cells/ml) were preincubated with NAC dissolved in Krebs–Henseleit buffer (final concentrations 1, 2.5, and 5 mM) for 20 min and with DCHF-DA dissolved in ethanol (final concentration 5 μM) for 15 min prior to the addition of $C_{60}(OH)_{24}$ at a concentration of 0.1 mM, respectively. After 1-h incubation, the hepatocyte suspensions were centrifuged at $100\times g$ for 5 min, and the fluorescence intensity in supernatant fraction (100 μl) obtained was measured in a CytoFluor 4000 multiwell fluorescence plate reader (PerSeptive Biosystems Inc., Framingham, MA, USA): The extinction and emission filters were set at 485 nm (bandwidth ±10 nm) and 530 nm (bandwidth ±12.5 nm), respectively. The results are expressed as percentages of the fluorescence values for the untreated hepatocytes.

Isolation of mitochondria from isolated rat hepatocytes

After the desired time of incubation with fullerenol and/or NAC, hepatocytes were collected by centrifugation at $100\times g$ for 5 min and homogenized with isolation medium (pH 7.4) containing 70 mM sucrose, 220 mM mannitol, 2.5 mM HEPES, 2 mM EDTA, and 0.1 mM phenylmethylsulfonyl fluoride in a Potter–Elvehjem glass homogenizer with a loose-fitting (clearance about 0.8 mm) Teflon pestle. (Cain and Skilleter 1987). After ten up-and-down strokes, the homogenate obtained was centrifuged at $2{,}000\times g$ for 10 min, and then, the resulting supernatant was centrifuged at $10{,}000\times g$ for 10 min to collect the mitochondrial pellet. The pellet was resuspended in the same medium and was centrifuged to obtain a more purified mitochondrial fraction in same condition again, and the mitochondrial pellet was finally suspended in the medium before measurement of GSH.

Statistical analysis

Statistical analysis was performed with a one-way analysis of variance, followed by Dunnett's or Duncan's multiple comparison test. Statistical significance was assumed at $p < 0.05$.

Results

Effects of NAC on $C_{60}(OH)_{24}$-induced toxicity in rat hepatocytes

To investigate the effects of NAC on $C_{60}(OH)_{24}$-induced cytotoxicity, rat hepatocytes were preincubated with NAC (1, 2.5, and 5 mM) for 20 min prior to the addition of the fullerenol at a concentration of 0.1 mM, a moderately toxic concentration (Nakagawa et al. 2011). As shown in Fig. 1, the exposure of isolated rat hepatocytes to $C_{60}(OH)_{24}$ caused time (0–3 h)-dependent cell death, as assayed by trypan blue dye exclusion, this was accompanied by a rapid depletion of the intracellular ATP level and formation of cell surface blebs. The determination of cellular ATP content rather than the trypan blue dye exclusion assay is a relatively sensitive assessment of cell viability (Stone et al. 2009). Despite this, $C_{60}(OH)_{24}$-induced cell death and ATP loss were effectively prevented by treatment with NAC ranging in concentration from 1 to 5 mM during the 3-h incubation period. The onset of the formation of plasma membrane blebs caused by the fullerenol was delayed by NAC at a concentration of 1 mM, whereas NAC at concentrations of greater than 2.5 mM prevented bleb formation.

Effects of NAC on $C_{60}(OH)_{24}$-induced intracellular levels of GSH, GSSG, reduced protein thiols, and MDA in rat hepatocytes

After 1 h of incubation with the fullerenol at a concentration of 0.1 mM, the intracellular GSH level was depleted rapidly, and the depletion of GSH was subsequently followed by an increase in glutathione disulfide (GSSG, glutathione-oxidized form) and a loss of reduced protein thiols with a significant increase in the cellular level of MDA, an index of lipid peroxidation, during the incubation period (Fig. 2).

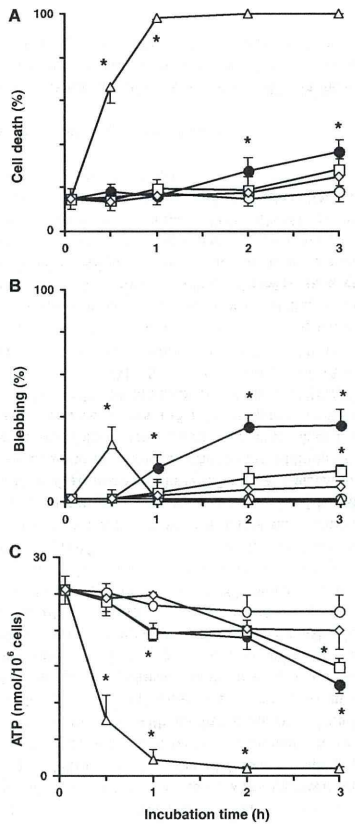

Fig. 1 Effects of NAC on cell death (**a**), blebbing (**b**), and intracellular level of ATP (**c**) in rat hepatocytes treated with $C_{60}(OH)_{24}$. Hepatocytes (10^6 cells/ml) were pretreated with different concentrations of NAC for 20 min prior to the addition of $C_{60}(OH)_{24}$ at a concentration of 0.1 mM, as described in "Materials and methods." No addition (*open circles*); $C_{60}(OH)_{24}$ alone (*open triangles*); NAC 1 mM plus $C_{60}(OH)_{24}$ 0.1 mM (*solid circles*); NAC 2.5 mM plus $C_{60}(OH)_{24}$ 0.1 mM (*open squares*); NAC 5 mM plus $C_{60}(OH)_{24}$ 0.1 mM (*open lozenges*). The results are expressed as mean ± SE of three separate experiments. *Significantly different from values for untreated (control) hepatocytes ($p < 0.05$)

On the other hand, NAC pretreatment prevented not only the decrease in the intracellular GSH and protein thiol levels, but also the increase in GSSG and MDA levels caused by $C_{60}(OH)_{24}$. NAC at concentrations of 2.5 and 5 mM in $C_{60}(OH)_{24}$-treated hepatocytes resulted in either high levels of GSH or simultaneously low levels of GSSG compared with those in untreated hepatocytes during the incubation period. After pretreatment of hepatocytes with NAC alone at concentrations of 1–5 mM, cellular GSH levels were slightly more than twofold those of untreated hepatocytes after 1-h incubation, whereas protein thiol levels were not affected by the addition of NAC (data not shown).

Changes in levels of NAC and its deacetylated intermediate, cysteine, in hepatocyte suspensions

To understand the metabolism of NAC in rat hepatocytes treated with $C_{60}(OH)_{24}$, time courses of changes in the levels of NAC and its deacetylated metabolite, free L-cysteine, were investigated (Fig. 3). The amounts of NAC and L-cysteine were quantified as described above, respectively. Although NAC itself was stable in Krebs–Henseleit buffer without hepatocytes during 3-h incubation (data not shown), initial levels (1, 2.5, and 5 mM) of NAC added to hepatocyte suspensions with $C_{60}(OH)_{24}$ decreased with time, accompanied by an increase in cellular levels of cysteine depending upon the initial concentration of NAC. Since the increase in intracellular GSH levels after the addition of NAC to hepatocyte suspensions was associated with an increase in free L-cysteine, this indicated that NAC was effectively deacetylated by isolated rat hepatocytes and is frequently employed as a source sulfhydryl group in hepatocytes as a precursor of GSH (Fig. 2). The rates of NAC loss and/or cysteine formation in hepatocytes were not affected by the presence/absence of the fullerenol during incubation (data not shown), indicating that the decrease in NAC level in hepatocyte suspensions was dependent on cellular hydrolytic (acylase) activity.

Effects of NAC on $C_{60}(OH)_{24}$-induced loss of mitochondrial membrane potential and generation of ROS in rat hepatocytes

The reduction in the cellular ATP levels caused by $C_{60}(OH)_{24}$ at a concentration of 0.1 mM was related to a decrease in the mitochondrial membrane potential (MMP; $\Delta\Psi$) to approximately 20 % of the control value after 45-min incubation (Fig. 4). On the other hand, MMP of hepatocytes preincubated with NAC at concentrations of 1 and 2.5 mM showed apparent protective effects against the loss of membrane potential caused by the fullerenol under the same conditions.

2′,7′-Dichlorodihydrofluorescein diacetate is widely used to measure ROS generation in various cells (Shen et al. 1996). Viable cells deacetylate DCHF-DA to 2′,7′-Dichlorodihydrofluorescein, which is not fluorescent,

Author's personal copy

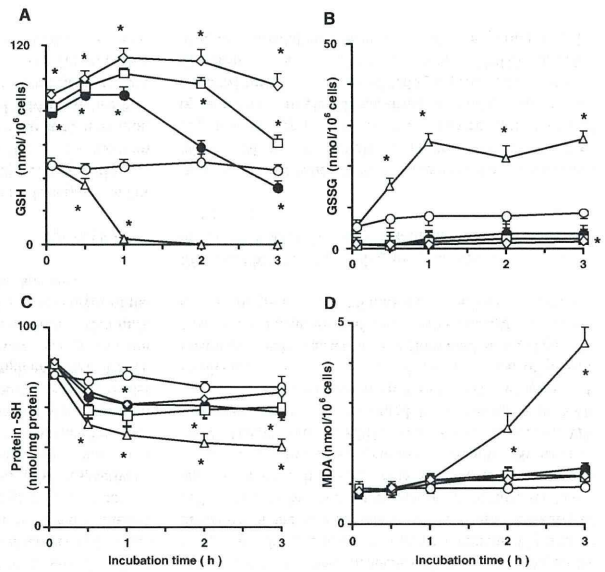

Fig. 2 Effects of NAC on intracellular levels of GSH (**a**), GSSG (**b**), protein thiols (**c**), and MDA (**d**) in isolated rat hepatocytes treated with $C_{60}(OH)_{24}$. Hepatocytes (10^6 cells/ml) were pretreated with different concentrations of NAC for 20 min prior to the addition of $C_{60}(OH)_{24}$ at a concentration of 0.1 mM, as described in "Materials and methods." No addition (*open circles*); $C_{60}(OH)_{24}$ alone (*open triangles*); NAC 1 mM plus $C_{60}(OH)_{24}$ 0.1 mM (*solid circles*); NAC 2.5 mM plus $C_{60}(OH)_{24}$ (*open squares*); NAC 5 mM plus $C_{60}(OH)_{24}$ (*open lozenges*). The results are expressed as mean ± SE of three separate experiments. *Significantly different from values for untreated (control) hepatocytes ($p < 0.05$)

but reacts quantitatively with ROS (H_2O_2 and O_2^-) within cells to form fluorescent dye, which remains trapped within the cells and can be measured to provide an index of intracellular oxidation. The levels of ROS following 1-h incubation with $C_{60}(OH)_{24}$ are shown in Fig. 5. The fluorescence intensity increased in hepatocytes incubated with $C_{60}(OH)_{24}$ at a concentration of 0.1 mM, but preincubation with NAC significantly prevented the increase in ROS levels.

Effects of NAC on $C_{60}(OH)_{24}$-induced mitochondrial GSH loss in rat hepatocytes

Mitochondrial GSH in hepatocytes is found mainly in the reduced form and represents a minor fraction of the total intracellular GSH pool (10–15 %) (Marí et al. 2009). Because previous studies indicated that mitochondria are target organelles for fullerenols (Nakagawa et al. 2011; Ueng et al. 1997), the effects of NAC on mitochondrial GSH levels in rat hepatocytes treated with $C_{60}(OH)_{24}$ at a concentration of 0.1 mM for 1 h were investigated (Fig. 6). In this study, mitochondrial pellets obtained by the first centrifugation from rat hepatocyte suspensions were centrifuged under the same conditions to obtain more purified mitochondria prior to the measurement of GSH. Although incubation of hepatocytes with $C_{60}(OH)_{24}$ resulted in a marked decrease in the mitochondrial GSH level, that loss was significantly prevented by the addition of NAC at concentrations of 1 and 2.5 mM. On the other hand, exposure of hepatocytes to NAC alone caused a concentration (1 and 2.5 mM)-dependent increase in the mitochondrial GSH level, which was approximately 1.8- and 2.5-fold greater than in the untreated (control) group (8.8 ± 1.1 nmol/mg protein; $n = 3$), respectively.

Effects of diethyl maleate (DEM) on rat hepatocytes treated with $C_{60}(OH)_{24}$

To investigate the effects of GSH depletion on $C_{60}(OH)_{24}$-induced cytotoxicity, rat hepatocytes were preincubated with DEM (1.25 mM), a GSH-depleting agent, for 15 min prior to the addition of the fullerenol at a concentration of 50 μM, a mildly toxic concentration. As shown in Fig. 7, severe depletion of cellular GSH levels occurred after preincubation with DEM led to the enhancement of cytotoxicity caused by the fullerenol, accompanied by a rapid loss of ATP levels and cell death. In addition, DEM treatment stimulated the formation of cell surface blebs caused by the fullerenol (data not shown). Although DEM at 1.25 mM elicited an abrupt depletion of the cellular GSH level, DEM

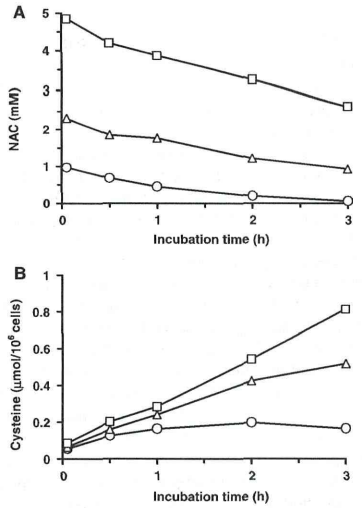

Fig. 3 Changes in the levels of NAC (**a**) and its deacetylated intermediate, L-cysteine (**b**), in rat hepatocyte suspensions. Hepatocytes (10^6 cells/ml) were preincubated with different concentrations of NAC for 20 min prior to the addition of $C_{60}(OH)_{24}$ at a concentration of 0.1 mM. The amounts of NAC and L-cysteine were determined as described in "Materials and methods." Initial concentrations of NAC added to hepatocyte suspensions were 1 mM (*open circles*), 2.5 mM (*open triangles*), and 5 mM (*open squares*). The increase in cysteine levels (**b**) depended upon the initial concentrations of NAC. The results are averages of two experiments

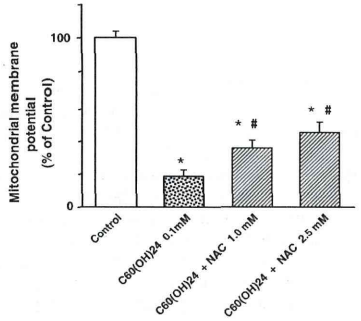

Fig. 4 Effects of NAC on the MMP in rat hepatocytes treated with $C_{60}(OH)_{24}$. Hepatocytes (10^6 cells/ml) were preincubated with different concentrations of NAC for 20 min prior to the incubation of $C_{60}(OH)_{24}$ 0.1 mM for 45 min and subsequently incubated with rhodamine 123 (1 μM) for 15 min as described in "Materials and methods." The results are expressed as mean ± SE of three determinations. *Significant difference from values for untreated (control) hepatocytes ($p < 0.05$). #Significant difference between $C_{60}(OH)_{24}$- and NAC plus $C_{60}(OH)_{24}$-treated hepatocytes ($p < 0.05$)

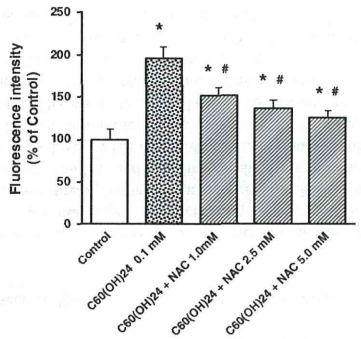

Fig. 5 Effects of NAC on ROS generation by $C_{60}(OH)_{24}$ in isolated rat hepatocytes. Hepatocytes (10^6 cells/ml) were preincubated with NAC (final concentrations 1, 2.5 and 5 mM) for 20 min and with DCHF-DA (5 μM) for 15 min and subsequently incubated with $C_{60}(OH)_{24}$ at a concentration of 0.1 mM for 1 h as described in "Materials and methods." The results are expressed as mean ± SE of three determinations. *Significant difference from values for untreated (control) hepatocytes ($p < 0.05$). #Significant difference between $C_{60}(OH)_{24}$- and NAC plus $C_{60}(OH)_{24}$-treated hepatocytes ($p < 0.05$)

itself caused neither cell death nor a decrease in cellular ATP level during the incubation period. Further, treatment with DEM did not induce lipid peroxidation (data not shown). This result indicates that the initial GSH level is an essential factor in the modulation of cytotoxicity observed in hepatocytes exposed to $C_{60}(OH)_{24}$.

Discussion

Effects of NAC on target sites of $C_{60}(OH)_{24}$-induced cytotoxicity

The results of the present study showed that in isolated rat hepatocytes, $C_{60}(OH)_{24}$ at a concentration of 0.1 mM elicited time-dependent acute cell death, which was accompanied by the formation of cell blebs and decreased in intracellular ATP levels and MMP (Figs. 1, 4). In our previous study, fullerenols such as $C_{60}(OH)_{12}$ and $C_{60}(OH)_{24}$ also elicited mitochondrial dysfunction related to oxidative phosphorylation and the MPT (Nakagawa et al. 2011). These results support the concept that mitochondria as an

Author's personal copy

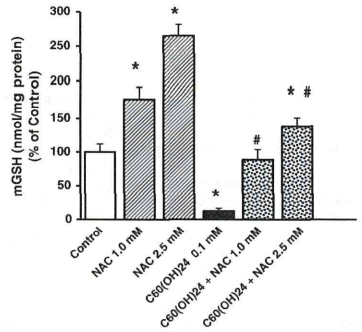

Fig. 6 Effects of NAC on mitochondrial GSH (mGSH) levels in rat hepatocytes treated with $C_{60}(OH)_{24}$. Hepatocytes (10^6 cells/ml) were preincubated with different concentrations of NAC for 20 min prior to incubation with $C_{60}(OH)_{24}$ 0.1 mM for 1 h, and subsequently mitochondria were collected by centrifugation followed by homogenization of hepatocytes. The amounts of mitochondrial GSH were determined as described in "Materials and methods." Values are expressed as mean ± SE of three determinations ($p < 0.05$). *Significant difference from values for untreated (control) hepatocytes ($p < 0.05$). #Significant difference between $C_{60}(OH)_{24}$- and NAC plus $C_{60}(OH)_{24}$-treated hepatocytes ($p < 0.05$)

ATP-generating site are important targets organelles for the fullerenol, resulting in energy stress caused by the rapid depletion of the cellular ATP pool. $C_{60}(OH)_{24}$-induced cell death was also initiated, at least in part, by oxidative stress, indicating that the depletion of cellular GSH caused by $C_{60}(OH)_{24}$ was concurrently associated with an increase in GSSG, MDA, and ROS levels, and a decrease in the levels of reduced protein thiol and mitochondrial GSH (Figs. 2, 5, 6). Despite these, the addition of NAC to rat hepatocyte suspensions effectively inhibited the cytotoxic and/or mitochondrial damage caused by $C_{60}(OH)_{24}$, suggesting the possibility that fullerenol-induced hepatotoxicity is ameliorated by the addition of NAC.

Previous in vitro studies about the subcellular distribution of nanomaterials showed that: (1) the water-soluble fullerene derivative $C_{61}(COOH)_2$ added to monkey kidney COS-7 cells was able to accumulate within the mitochondria through the cell membrane and preferentially affected mitochondrial function such as its electron transport chain (Foley et al. 2002); and (2) when nanoparticles consisting of organic carbon and polycyclic aromatic hydrocarbons were incorporated by macrophages and/or epithelial cells, they localized in the mitochondria and induced structural damage through oxidative stress (Li et al. 2003). Mitochondrial structural damage caused by fullerenols is supported by our previous results showing that fullerenols, especially

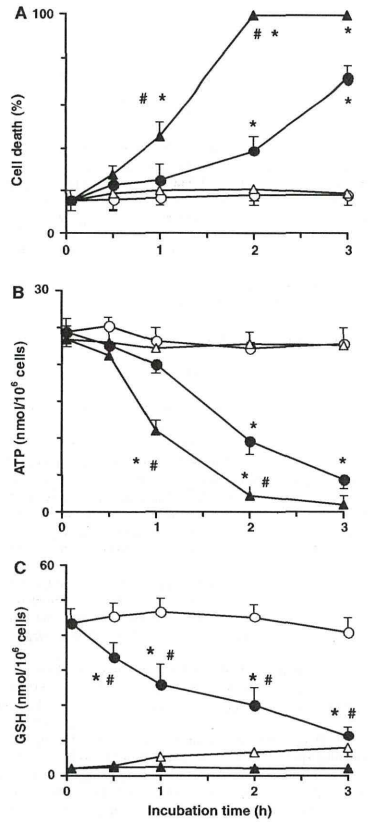

Fig. 7 Effects of DEM on cell death (**a**) and intracellular levels of ATP (**b**) and GSH (**c**) in isolated rat hepatocytes treated with $C_{60}(OH)_{24}$. Hepatocytes (10^6 cells/ml) were preincubated with DEM 1.25 mM for 15 min prior to the addition of $C_{60}(OH)_{24}$ at a concentration of 50 μM, as described in "Materials and methods." No addition (*open circles*); DEM alone (*open triangles*); $C_{60}(OH)_{24}$ alone (*solid circles*); DEM plus $C_{60}(OH)_{24}$ (*solid triangles*). The results are expressed as mean ± SE of three separate experiments. *Significantly different from values for untreated (control) hepatocytes ($p < 0.05$). #Significant difference between $C_{60}(OH)_{24}$- and DEM plus $C_{60}(OH)_{24}$-treated hepatocytes ($p < 0.05$)

$C_{60}(OH)_{24}$, resulted in the induction of organelle swelling, as assayed by the mitochondrial MPT which was monitored by the absorbance changes at 540 nm (Nakagawa et al. 2011). It is well known that the homeostasis of MMP

is disturbed by chemicals and/or xenobiotics (Lemasters et al. 1993). In addition, the depletion of intracellular ATP caused by xenobiotics is known to be a critical factor in the development of plasma membrane blebbing prior to cell death (Nicotera et al. 1992), and the maintenance of cellular ATP levels is necessary for the polymerization of microfilaments and microtubules, which is related to the interaction between the cytoskeletal organization and cellular morphology (Bellomo et al. 1990). In this regard, Johnson-Lyles et al. (2010) observed that in LLC-PK1 cells, the fullerenol $C_{60}(OH)_n$ caused cytotoxicity through depletion of the intracellular ATP levels accompanied by cytoskeletal disruption. After the exposure of rat hepatocytes to $C_{60}(OH)_{24}$, the onset of bleb formation associated with the depletion of cellular ATP levels was effectively prevented by pretreatment with NAC (Fig. 1). In this connection, Zaragoza et al. (2001) observed that cocaine-induced cytotoxicity via mitochondrial damage was prevented by NAC pretreatment in rat hepatocytes. Based on the results of previous and the present studies, it seems that $C_{60}(OH)_{24}$ penetrates the hepatocyte membrane and accumulates in mitochondria to elicit organelle dysfunction, which could be effectively attenuated by pretreatment with NAC.

Metabolism of NAC and its effects on $C_{60}(OH)_{24}$-induced cytotoxicity

Freshly isolated rat hepatocytes retain intact membranes and have high levels of various drug-metabolizing enzymes and their cofactors associated with phase I and phase II reactions, and multiple defense systems against intracellular oxidative stress produced by various chemicals (Moldéus et al. 1978). As shown in Fig. 3, the amounts of NAC added to hepatocyte suspensions decreased rapidly with time, accompanied by an increase in cysteine levels, indicating that NAC incorporated into hepatocytes was enzymatically *N*-deacetylated by cytosolic aminoacylase and was frequently employed as a source sulfhydryl group in hepatocytes as a precursor of GSH (Fig. 2), which is well known as a major antioxidant and free radical scavenger that protects cells from ROS in isolated rat hepatocytes and other cell lines treated with drugs and xenobiotics (Reed 1990; Nakagawa et al. 2005; Marí et al. 2009). When NAC led to the enhancement of cellular and mitochondrial levels of GSH (Figs. 2, 6), $C_{60}(OH)_{24}$-induced ROS generation and MMP loss were apparently prevented (Figs. 4, 5). Despite this, a certain amount of NAC incorporated into hepatocytes may also reduce free radical species, because Zhang et al. (2011) reported that in renal proximal tubule epithelial cells exposed to a hydroquinone derivative, NAC may exert cytoprotective effects in part by directly scavenging ROS. It was observed that the ability of cysteine to react with ROS was less than that of NAC in a phosphate buffer without cells (Aruoma et al. 1989), while free cysteine produced in rat hepatocytes as shown in Fig. 3 cannot be disregarded as an effective antioxidant and/or a protector of thiols (Takashima et al. 2012). Pretreatment of rat hepatocyte suspensions with L-cysteine is known to prevent the decrease in cellular levels of GSH and protein thiols caused by hydroxylated biphenyls (Nakagawa et al. 1992). The accumulation of proteins with irreversible thiol oxidation, which is a hallmark of oxidative stress-induced cellular damage (Kettenhofen and Wood 2010), caused by $C_{60}(OH)_{24}$ was also prevented by the addition of NAC (Fig. 2). Since the mechanism of fullerenol-induced oxidative stress within hepatocytes may be attributed to a sulfhydryl redox-state imbalance, further studies are necessary to determine the multiple defense systems of NAC.

Effects of NAC on mitochondrial toxicity induced by $C_{60}(OH)_{24}$

Because mitochondria in hepatocytes, as in other organ cells, are the main site of energy production, their dysfunction directly/indirectly affects cellular ATP synthesis and cell viability, and thus, the mechanisms of cytotoxicity caused by a wide range of chemicals and a number of pathologic conditions (Kehrer et al. 1990; Wallace et al. 1997). The synthesis of GSH from its constituent amino acids, cysteine, glutamate, and glycine involves two ATP-requiring enzymatic systems and thus depends on the continuous supplementation of ATP. The distribution of reduced GSH in the cytosolic and mitochondrial fractions is approximately 85–90 and 10–15 %, respectively (Marí et al. 2009). It is well known that GSH can easily cross the mitochondrial outer membrane via porin channels and the mitochondrial inner membrane (Smith et al. 1996). Thus, the mitochondrial GSH level depends on (1) cytosol mitochondrial level and (2) specific transporters on the mitochondrial membrane. In this study, the loss of the MMP caused by $C_{60}(OH)_{24}$ was partially recovered after NAC addition in a concentration-dependent manner, accompanied by the restoration of depleted mitochondrial GSH levels (Figs. 4, 6). Because NAC may exert cytoprotective effects by increasing the mitochondrial GSH level, alterations in the GSH pool may also participate in the mitochondrial bioenergetics of fullerenol-treated hepatocytes. On the other hand, pretreatment with DEM (1.25 mM), which caused an abrupt depletion of cytosolic and mitochondrial GSH levels and did not elicit cytotoxicity (Ku and Billings 1986), enhanced $C_{60}(OH)_{24}$-induced cytotoxicity, suggesting that intracellular factors, especially the mitochondrial reduced GSH pool, play an important role in the onset of cytotoxicity (Fig. 7). Several studies concluded that exposure to most chemicals exposures is associated with the depletion of mitochondrial GSH rather than cytosolic GSH

Author's personal copy

to regulate the apoptotic pathway (Mithöfer et al. 1992; Lluis et al. 2005; Fernandez-Checa and Kaplowitz 2005). In addition, mitochondrial GSH is also a critical factor regulating the redox status of protein thiols that regulate the mitochondrial MPT (Chernyak and Bernardi 1996; Armstrong and Jones 2002), the disturbance of which is induced by hydroxylated fullerenes. Therefore, the finding that NAC elicits increases in the levels of mitochondrial GSH as well as cytosolic GSH in rat hepatocytes suggests that maintenance of the mitochondrial GSH level could prevent, at least partially, mitochondrial dysfunction such as ATP generation caused by the fullerenol.

Mitochondria are also the major source of the generation of toxic ROS, which is enhanced by the actions of various mitochondrial inhibitors from complexes I to IV (Mehta et al. 2008; Zhang et al. 2001). Although it is uncertain whether the generation of ROS in hepatocytes incubated with $C_{60}(OH)_{24}$ depends on disturbance of the mitochondrial respiration chain, fullerenols are known to be free radical scavengers and/or antioxidants in biological systems (Dugan et al. 1996; Kamat et al. 2000; Saitoh et al. 2010). Further investigations are necessary to clarify the mechanisms of their harmful and/or protective effects and to study nanomaterial-biological interactions.

In conclusion, the results of the current study show that the exposure of hepatocytes to $C_{60}(OH)_{24}$ caused cytotoxicity, accompanied by losses of intracellular ATP, GSH, and protein thiols, and an increase in GSSG and ROS levels. On the other hand, NAC ameliorated (a) mitochondrial dysfunction linked to the depletion of ATP and the MMP and (b) induction of oxidative stress as assessed by ROS generation, losses of cellular and/or mitochondrial GSH and protein thiol levels, and MDA formation. NAC taken up hepatocytes was effectively converted to GSH through deacetylated cysteine. The cytotoxicity caused by the fullerenol was enhanced by the addition of DEM, which continuously depleted cellular GSH. Taken collectively, these results indicate that the onset of the toxic effects of $C_{60}(OH)_{24}$ is, at least in part, affected by intracellular and/or mitochondrial GSH levels as well as mitochondrial dysfunction.

References

Albano E, Rundgren M, Hervison PJ, Nelson SD, Moldéus P (1985) Mechanisms of *N*-acetyl-*p*-benzoquinone imine cytotoxicity. Mol Pharmacol 28:306–311

Armstrong JS, Jones DP (2002) Glutathione depletion enforces the mitochondrial permeability transition and causes cell death in Bcl-2 overexpressing HL60 cells. FASEB J 16:1263–1265

Aruoma OI, Halliwell B, Hoey BM, Butler J (1989) The antioxidant action of *N*-acetylcysteine: its reaction with hydrogen peroxide, hydroxyl radical, superoxide, and hypochlorous acid. Free Radic Biol Med 6:593–597

Bellomo G, Mirabelli F, Richelmi P, Malorni W, Iosi F, Orrenius S (1990) The cytoskeleton as a target in quinone toxicity. Free Radic Res Commun 8:391–399

Bogdanović G, Kojić V, Dordević A, Canadanović-Brunet J, Vojinović-Miloradov M, Baltić VV (2004) Modulating activity of fullerols $C_{60}(OH)_{22}$ on doxorubicin-induced cytotoxicity. Toxicol In Vitro 18:629–637

Borm PJA, Robbins D, Haubold S, Kuhlbusch T, Fissan H, Donaldson K, Schins R, Stone V, Kreyling W, Lademann J, Krutmann J, Warheit D, Oberdorster E (2006) The potential risks of nanomaterials: a review carried out for ECETOC. Part Fibre Toxicol 3:11. doi:10.1186/1743-8977-3-11

Cain K, Skilleter DS (1987) Preparation and use of mitochondria in toxicological research. In: Snell K, Mullock B (eds) Biochemical toxicology—A practical approach. IRL, Oxford, pp 217–254

Chen YW, Hwang KC, Yen CC, Lai YL (2004) Fullerene derivatives protect against oxidative stress in RAW 264.7 cells and ischemia-reperfused lungs. Am J Physiol Regul Integr Comp Physiol 287:R21–R26

Chen C, Xing G, Wang J, Zhao F, Chai Z, Fang X (2005) Multihydroxylated $[Gd@C_{82}(OH)_{22}]_n$ nanoparticles: antineoplastic activity of high efficiency and low toxicity. Nano Lett 5:2050–2057

Chernyak BV, Bernardi P (1996) The mitochondrial permeability transition pore is modulated by oxidative agents through both pyridine nucleotides and glutathione at two separate sites. Eur J Biochem 238:623–630

Dugan LL, Gabrielsen JK, Yu SP, Lin TS, Choi DW (1996) Buckminsterfullerenol free radical scavengers reduce excitotoxic and apoptotic death of cultured cortical neurons. Neurobiol Dis 3:129–135

Fernandez-Checa JC, Kaplowitz N (2005) Hepatic mitochondrial glutathione: transport and role in disease and toxicity. Toxicol Appl Pharmacol 204:263–273

Foley S, Crowley C, Smaihi M, Bonfils C, Erlanger BF, Seta P, Larroque C (2002) Cellular localization of a water-soluble fullerene derivative. Biochem Biophys Res Commun 294:116–119

Hinchman CA, Matsumoto H, Simmons T, Ballatori N (1991) Intrahepatic conversion of a glutathione conjugate to its mercapturic acid. Metabolism of 1-chloro-2,4-dinitrobenzne in isolated perfused rats and guinea pig livers. J Biol Chem 266:22179–22185

Hoet PHM, Brüske-Hohlfeld I, Salata O (2004) Nanoparticles-known and unknown health risks. J Nanobiotechnol 2:1–15

Injac R, Perse M, Obermajer N, Djordjevic-Milic V, Prijatelj M, Djordjevic A, Cerar A, Strukelj B (2008) Potential hepatoprotective effects of fullerenol $C_{60}(OH)_{24}$ in doxorubicin-induced hepatotoxicity in rats with mammary carcinomas. Biomaterials 29:3451–3460

Injac R, Radic N, Govedarica B, Perse M, Cerar A, Djordjevic A, Strukelj B (2009) Acute doxorubicin pulmotoxicity in rat with malignant neoplasm is effectively treated with fullerenol $C_{60}(OH)_{24}$ through inhibition of oxidative stress. Pharmacol Rep 61:335–342

Isakovic A, Markovic Z, Todorovic-Markovic B, Nikolic N, Vranjes-Djuric S, Mirkovic M, Dramicanin M, Harhaji L, Raicevic N, Nikolic Z, Trakovic V (2006) Distinct cytotoxic mechanisms of pristine versus hydroxylated fullerene. Toxicol Sci 91:173–183

Jin H, Chen WQ, Tang XW, Chiang LY, Yang CY, Schloss JV, Wu JY (2000) Polyhydroxylated C_{60}, fullerenols, as glutamate receptor antagonists and neuroprotective agents. J Neurosci Res 62:600–607

Johnson-Lyles DN, Peifley K, Lockett S, Neun BW, Hansen M, Clogston J, Stern ST, McNeil SE (2010) Fullerenol cytotoxicity in kidney cells is associated with cytoskeleton disruption, autophagic vacuole accumulation, and mitochondrial dysfunction. Toxicol Appl Pharmacol 248:249–258

Jones DP (1981) Determination of pyridine dinucleotides in cell extracts by high-performance liquid chromatography. J Chromatogr 225:446–449

Kamat JP, Devasagayam TP, Priyadarsini KI, Mohan H (2000) Reactive oxygen species mediated membrane damage induced by fullerene derivatives and its possible biological implications. Toxicology 155:55–61

Kehrer JP, Jones DP, Lemasters JJ, Farber H, Jaeschke H (1990) Mechanisms of hypoxic cell injury. Summary of the symposium presented at the 1990 annual meeting of the society of toxicology. Toxicol Appl Pharmacol 106:165–178

Kettenhofen NJ, Wood MJ (2010) Formation, reactivity, and detection of protein sulfenic acids. Chem Res Toxicol 23:1633–1646

Kroto HW, Heath JR, O'Brien SC, Curl RF, Smalley RE (1985) C_{60}: buckminsterfullerene. Nature 318:162–163

Ku RH, Billings RE (1986) The role of mitochondrial glutathione and cellular protein sulfhydryls in formaldehyde toxicity in glutathione-depleted rat hepatocytes. Arch Biochem Biophys 247:183–189

Lemasters JJ, Nieminen AL, Chacon E, Imberti R, Gores G, Reece JM, Herman B (1993) Use of fluorescent probes to monitor mitochondrial membrane potential in isolated mitochondria, cell suspensions, and cultured cells. In: Lash LH, Jones DP (eds) Mitochondrial dysfunction. Academic, San Diego, pp 404–415

Li N, Sioutas C, Cho A, Schmitz D, Misra C, Sempf J, Wang M, Oberley T, Froines J, Nel A (2003) Ultrafine particulate pollutants induce oxidative stress and mitochondrial damage. Environ Health Percept 111:455–460

Lluis JM, Morales A, Blasco C, Colell A, Mari M, Garcia-Ruiz C, Fernandez-Checa JC (2005) Critical role of mitochondrial glutathione in the survival of hepatocytes during hypoxia. J Biol Chem 280:3224–3232

Lowry OH, Rosebrough NJ, Farr AL, Randall RJ (1951) Protein measurement with the Folin phenol reagent. J Biol Chem 193:265–275

Marí M, Morales A, Colell A, García-Ruiz C, Fernández-Checa JC (2009) Mitochondrial glutathione, a key survival antioxidant. Antioxid Redox Signal 11:2685–2700

Mehta R, Chan K, Lee O, Tafazoli S, O'Brien PJ (2008) Drug-associated mitochondrial toxicity. In: Dykens JA, Will Y (eds) Drug-induced mitochondrial dysfunction. Wiley, Hoboken, pp 71–126

Mithöfer K, Sandy MS, Smith MT, Di Monte D (1992) Mitochondrial poisons cause depletion of reduced glutathione in isolated hepatocytes. Arch Biochem Biophys 295:132–136

Moldéus P, Hogberg J, Orrenius S (1978) Isolation and use of liver cells. Methods Enzymol 52:60–71

Mrdanović J, Solajić C, Bogdanović V, Stankov K, Bogdanović G, Djordjevic A (2009) Effects of fullerenol $C_{60}(OH)_{24}$ on the frequency of micronuclei and chromosome aberrations in CHO-K1 cells. Mutat Res 680:25–30

Murugan MA, Gangadharan B, Mathur P (2002) Antioxidative effect of fullerenol on goat epididymal spermatozoa. Asian J Androl 4:149–152

Nakagawa Y, Tayama S, Moore GA, Moldéus P (1992) Relationship between metabolism and cytotoxicity of *ortho*-phenylphenol in isolated rat hepatocytes. Biochem Pharmacol 43:1431–1437

Nakagawa Y, Tayama S, Moore G, Moldéus P (1993) Effect of diethyl maleate on phenyl-hydroquinone-induced cytotoxicity in isolated rat hepatocytes. Xenobiotica 23:205–213

Nakagawa Y, Suzuki T, Kamimura H, Nagai F (2005) *N*-nitrosofenfluramine induces cytotoxicity via mitochondrial dysfunction and oxidative stress in isolated rat hepatocytes. Arch Toxicol 79:312–320

Nakagawa Y, Suzuki T, Ishii H, Nakae D, Ogata A (2011) Cytotoxic effects of hydroxylated fullerenes on isolated rat hepatocytes via mitochondrial dysfunction. Arch Toxicol 85:1429–1440

Nicotera P, Bellomo G, Orrenius S (1992) Calcium-mediated mechanisms in chemically induced cell death. Annu Rev Pharmacol Toxicol 32:449–470

Niwa Y, Iwai N (2007) Nanomaterials induce oxidized low-density lipoprotein cellular uptake in macrophages and platelet aggregation. Circ J 71:437–444

Pombrio JM, Giangreco A, Li L, Wempe MF, Anders MW, Sweet DH, Pritchard JB, Ballatori N (2001) Mercapturic acid (*N*-acetylcysteine *S*-conjugates) as endogenous substrates for the renal organic anion transporter-1. Mol Pharmacol 60:1091–1099

Reed DJ (1990) Glutathione: toxicological implications. Annu Rev Pharmacol Toxicol 30:603–631

Reed DJ, Babson JR, Beatty PW, Brodie AE, Ellis WW, Potter DW (1980) High-performance liquid chromatography analysis of nanomole levels of glutathione, glutathione disulfide and related thiols and disulfides. Anal Biochem 106:55–62

Roberts JE, Wielgus AR, Boyes WK, Andley U, Chignell CF (2008) Phototoxicity and cytotoxicity of fullerol in human lens epithelial cells. Toxicol Appl Pharmacol 228:49–58

Sadauskas E, Wallin H, Stoltenberg M, Vogel U, Doering P, Larsen A, Danscher G (2007) Kupffer cells are central in the removal of nanoparticles from the organism. Part Fibre Toxicol 4:10. doi:10.1186/1743-8911-4-10

Saitoh Y, Xiao L, Mizuno H, Kato S, Aoshima H, Taira H, Kokubo K, Miwa N (2010) Novel polyhydroxylated fullerene suppresses intracellular oxidative stress together with repression of intracellular lipid accumulation during the differentiation of OP9 preadipocytes into adipocytes. Free Radic Res 44:1072–1081

Sandy MS, Moldéus P, Ross D, Smith M (1986) Role of redox cycling and lipid peroxidation in bipyridyl herbicide cytotoxicity. Studies with a compromised isolated hepatocyte model system. Biochem Pharmacol 35:3095–3101

Sayes CM, Fortner JD, Guo W, Lyon D, Boyd AM, Ausman KD, Tao YJ, Sitharaman B, Wilson LJ, Hughes JB, West JL, Colvin VL (2004) The differential cytotoxicity of water-soluble fullerenes. Nano Lett 4:1881–1887

Shen H-M, Shi C-Y, Shen Y, Ong C-N (1996) Detection of elevated reactive oxygen species level in cultured rat hepatocytes treated with aflatoxin B_1. Free Radic Biol Med 21:139–146

Smith CV, Jones DP, Guenthner TM, Lash LH, Lauterburg BH (1996) Compartmentation of glutathione: implications for the study of toxicity and disease. Toxicol Appl Pharmacol 140:1–12

Stone V, Johnston H, Schins RP (2009) Development of in vitro systems for nanotoxicology: methodological considerations. Crit Rev Toxicol 39:613–626

Takashima M, Shichiri M, Hagihara Y, Yoshida Y, Niki E (2012) Reactive toward oxygen radicals and antioxidant action of thiol compounds. Biofactors 38:240–248

Tirmenstein MA, Nicholls-Grzemski FA, Zhang JG, Fariss MW (2000) Glutathione depletion and the production of reactive oxygen species in isolated hepatocyte suspensions. Chem Biol Interact 127:201–217

Tsai MC, Chen YH, Chiang LY (1997) Polyhydroxylated C_{60}, fullerenol, a novel free-radical trapper, prevented hydrogen peroxide- and cumene hydroperoxide-elicited changes in rat hippocampus in vitro. J Pharm Pharmacol 49:438–445

Ueng T-H, Kang-JJ Wang HW, Cheng-YW Chiang LY (1997) Suppression of microsomal cytochrome P450-dependent monooxygenases and mitochondrial oxidative phosphorylation by fullerenol, a polyhydroxylated fullerene C_{60}. Toxicol Lett 93:29–37

Wallace KB, Eells JT, Madeira VM, Cortopassi G, Jones DP (1997) Mitochondria-mediated cell injury. Symposium overview. Fundam Appl Toxicol 38:23–37

Wang H, Joseph JA (1999) Quantifying cellular oxidative stress by dichlorofluorescein assay using microplate reader. Free Radic Biol Med 27:612–616

Author's personal copy

Yamawaki H, Iwai N (2006) Cytotoxicity of water-soluble fullerene in vascular endothelial cells. Am J Physiol Cell Physiol 290:C1495–C1502

Zafarullah M, Li WQ, Sylvester J, Ahmad M (2003) Molecular mechanisms of *N*-acetylcysteine actions. Cell Mol Life Sci 60:6–20

Zaragoza A, Díez-Fernández C, Alvarez AM, Andés D, Cascales M (2001) Mitochondrial involvement in cocaine-treated rat hepatocytes: effect of *N*-acetylcysteine and deferoxamine. Br J Pharmacol 132:1063–1070

Zhang JG, Tirmenstein MA, Nicholls-Grzemski FA, Fariss NW (2001) Mitochondrial electron transport inhibitors cause lipid peroxidation-dependent and -independent cell death: protective role of antioxidants. Arch Biochem Biophys 393:87–96

Zhang F, Lau SS, Monks TJ (2011) The cytoprotective effect of *N*-acetyl-L-cysteine against ROS-induced cytotoxicity is independent of its ability to enhance glutathione synthesis. Toxicol Sci 120:87–97

Int. J. Mol. Sci. **2011**, *12*, 3705-3722; doi:10.3390/ijms12063705

OPEN ACCESS

International Journal of
Molecular Sciences
ISSN 1422-0067
www.mdpi.com/journal/ijms

Review

Application of Magnetic Nanoparticles to Gene Delivery

Daisuke Kami [1,*], Shogo Takeda [2], Yoko Itakura [1], Satoshi Gojo [1], Masatoshi Watanabe [2] and Masashi Toyoda [1]

[1] Research Team for Vascular Medicine, Tokyo Metropolitan Institute of Gerontology, 35-2 Sakae-cho, Itabashi-ku, Tokyo 173-0015, Japan; E-Mails: yitakura@tmig.or.jp (Y.I.); satoshigojo-tky@umin.ac.jp (S.G.); mtoyoda@tmig.or.jp (M.T.)

[2] Laboratory for Medical Engineering, Division of Materials and Chemical Engineering, Yokohama National University, 79-1 Tokiwadai, Hodogaya-ku, Yokohama 240-8501, Japan; E-Mails: smilesnow1987@gmail.com (S.T.); mawata@ynu.ac.jp (M.W.)

* Author to whom correspondence should be addressed; E-Mail: dkami@tmig.or.jp; Tel.: +81-3-3964-3241; Fax: +81-3-3579-4776.

Received: 6 May 2011; in revised form: 18 May 2011 / Accepted: 25 May 2011 / Published: 7 June 2011

Abstract: Nanoparticle technology is being incorporated into many areas of molecular science and biomedicine. Because nanoparticles are small enough to enter almost all areas of the body, including the circulatory system and cells, they have been and continue to be exploited for basic biomedical research as well as clinical diagnostic and therapeutic applications. For example, nanoparticles hold great promise for enabling gene therapy to reach its full potential by facilitating targeted delivery of DNA into tissues and cells. Substantial progress has been made in binding DNA to nanoparticles and controlling the behavior of these complexes. In this article, we review research on binding DNAs to nanoparticles as well as our latest study on non-viral gene delivery using polyethylenimine-coated magnetic nanoparticles.

Keywords: magnetic nanoparticles; Magnetofection; gene delivery; polyethylenimine

1. Introduction

Nanotechnology describes the creation and utilization of materials, devices, and systems through the control of nanometer-sized materials and their application to physics, chemistry, biology, engineering, materials science, medicine, and other endeavors. In particular, intensive efforts are in progress to develop nanomaterials for medical use as agents that can be targeted to specific organs, tissues, and cells. For example, magnetic nanoparticles (MNPs) are being used clinically as contrast agents for magnetic resonance imaging (MRI) (Table 1). MRI is a noninvasive technique that can provide real-time high-resolution soft tissue information [1,2]. MRI image quality can be further improved by utilizing contrast agents that alter proton relaxation rates [3–8]. MNP-based drug delivery systems (DDS) [9–11], and treatments of hyperthermia [12–21], using MNPs have been studied for over a decade. Furthermore, researchers have reported that MNPs have been useful in hyperthermic treatment for various cancers *in vivo* [22–31]. Nanotechnology-based anti-cancer agent DDS have already been approved, such as pegylated liposomal doxorubicin (DOXIL) for ovarian cancer [32–37]. MNPs have been used effectively as transfection reagents for introducing nucleic acids (plasmids or siRNAs) [38–53], or viruses (retrovirus, or adenovirus) [44,54–56] into cells. Our own research is focused on MNP-mediated gene delivery systems (called as "Magnetofection").

Table 1. Biomedical Applications of Magnetic Nanoparticles (MNPs).

	Purpose	References
MRI	Diagnosis	[1–8,57–61]
DDS	Anti-cancer therapy, Enzyme therapy	[9–11,22–31]
Hyperthermia	Anti-cancer therapy	[12–18,33–37]
Gene Delivery	Anti-cancer therapy, Cell transplantation therapy	[38–55]

2. Gene Delivery

Gene delivery techniques efficiently introduce a gene of interest in order to express its encoded protein in a suitable host or host cell. Currently, there are three primary gene delivery systems that employ viral vectors (retroviruses and adenoviruses), nucleic acid electroporation, and nucleic acid transfection. These systems vary in efficacy (Table 2). Gene delivery by viral vectors can be highly efficient (80–90%) but may insert viral vector nucleic acid sequences into the host genome, potentially causing unwelcome effects, such as inappropriate expression of deleterious genes. Electroporation is also a highly efficient technique for introducing foreign genes into a host (50–70%); however, half of the recipient cells die due to the electrical stimulation. Transfection reagents do not efficiently deliver nucleic acids into cells (20–30%); however, cell viability is largely preserved and the method is safe enough for clinical use. Therefore, this method holds relatively more promise for medical applications, provided that its efficiency can be improved. MNPs are already in use by basic researchers to increase transfection efficiencies of cultured cells. Thus, MNP-nucleic acid complexes are added to cell culture media and then onto the cell surface by applying a magnetic force (Figure 1).

Table 2. Gene delivery systems.

	Expression Type	Efficiency (%)	Cell Viability (%)	Safety
Virus *	Stable, or Transient	80–90%	80–90%	Low
Electroporation	Transient	50–70%	40–50%	High
TF reagent **	Transient	20–30%	80–90%	High

* Virus including adenovirus (transient), retrovirus (stable), and lentivirus (stable); ** TF reagent, transfection reagents including PEI (Polysciences Inc.), FuGENE HD (Promega), and Lipofectamine 2000 (Invitrogen); All values are ours (unpublished experiments).

Figure 1. MNP gene delivery system (Magnetofection). Plasmids are bound to MNPs, which then move from the media to the cell surface by applying a magnetic force.

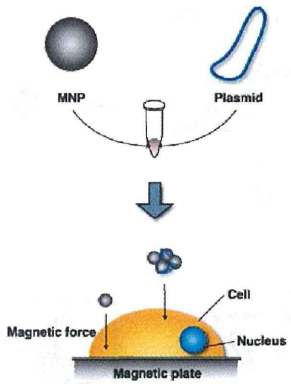

Oxide nanoparticles mixed with high magnetic moment compounds such as $CoFe_2O_4$, $NiFe_2O_4$, and $MnFe_2O_4$ exhibit superior performance compared to other magnetic materials [62,63]. However, these nanoparticles are highly toxic to cells, limiting their use for *in vivo*, and *in vitro* biomedical applications [64–67]. However, iron oxides such as magnetite (Fe_3O_4) and maghemite (γ-Fe_2O_3), in particular, possess high magnetic moments, are relatively safe, and currently in clinical use as MRI contrast agents [57–61]. These iron oxide based-magnetic materials are also suitable for biomedical applications. Fe^{3+} is widely dispersed in the human body so leaching of this metal ion from nanoparticles should not reach toxic concentrations [68,69]. As a result, maghemite is a popular choice for MNPs used biomedical applications. It is very important to modify the surface of MNPs so that they can be used for biomedical applications. Thus, MNPs are coated with compounds such as natural polymers (proteins and carbohydrates) [70–75], synthetic organic polymers (polyethylene glycol), polyvinyl alcohol, poly-L-lactic acid) [72,76–78], silica [79], and gold [80,81]. These surface coating agents prevent nanoparticle agglomeration, cytotoxicity, and add functionality. MNPs agglomerate readily in aqueous solutions around pH 7 [82], and it is difficult to control the properties and amounts of agglomerated MNPs. The greater toxicity of MNPs compared to those of microparticles can be attributed to their high surface to volume ratio [83]. Coating agents prevent the leaching of potentially toxic components from MNPs. In fact, the cytotoxicity of uncoated $NiFeO_4$ MNPs is dramatically

decreased by coating with cationic polymer, polyethylenimine (PEI) [84–86]. PEI, a cationic polymer, is widely used for nucleic acid transfection [87–89] and also serves as a nanoparticle dispersant [90]. PEI-coated MNPs enhance transfection efficiency [38,41,42,44–46,48,49,51,54,55].

3. Cell Transplantation Therapy Using MNPs

Autologous cell transplantation has been widely used in the clinic for decades. Delivering therapeutic genes to patients using their own cells avoids using immunosuppressive drugs. We reasoned, therefore, that a non-viral gene delivery system using iron oxide-based MNPs could provide a powerful tool for next-generation therapies. Gene delivery using MNPs has been successful for delivering nucleic acids into living cells with high efficiency and low cytotoxicity [38,41,42,44–46,48,49,51,54,55]. Currently, there are several methods for inducing cellular differentiation.

One of these methods, termed direct reprogramming, or direct conversion, has successfully yielded induced cardiomyocytes, induced neurons, reprogrammed pancreatic β cells, and induced pluripotent stem cells (iPSCs) [91–95]. Direct reprogramming represents a more straightforward strategy to treat diseases involving loss of function by specific cell populations compared to approaches requiring an intermediate embryonic stem cell. Thus, patient-derived differentiated cells by gene transfer are suitable for autologous cell transplantation, potentially resulting in faster patient recoveries. The scheme is classified into *ex vivo* gene therapy. The steps involved in this technique are as follows: (1) Patient-derived cells (such as fibroblasts) are cultured in chemically defined media *in vitro*; (2) These cells are transfected by MNPs, and differentiated into functional cells; (3) Differentiated cells are isolated by fluorescence-activated cell sorting (FACS); (4) FACS-purified differentiated cells are transplanted into the patient's target tissue (Figure 2).

Here we briefly describe the magnetofection [96], and our latest study concerning non-viral gene delivery using deacylated polyethylenimine coated MNPs.

Figure 2. Strategy for cell transplantation therapy. A patient's cells are cultured in chemically defined media. MNP-transfected cells by the introduced gene are isolated by FACS. FACS-purified differentiated cells are transplanted into the patient.

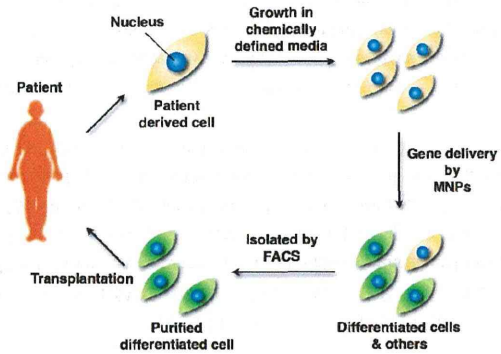

4. Gene Delivery Using MNPs and Magnetic Force

The mechanism of magnetofection is similar to using transfection reagents (Lipofectamine 2000, FuGENE HD, and PEI). The only difference is that the plasmids form complexes with cationic polymer-coated MNPs (called as "Magnetoplex") [42,48,97–99] (Figure 3). Figure 3 shows the two difference techniques. The behavior of magnetoplex is readily controlled by magnetic force. Upon binding to the cell surface they are taken up by endocytosis [51,100,101]. Thus, the transfection efficiency was increased.

Figure 3. Gene delivery systems using a transfection reagent (cationic polymer) and MNPs: (**A**) Gene delivery system using transfection reagent. The polyplex moves randomly in culture medium; (**B**) Magnetofection system. The magnetoplex only moves to the cell surface.

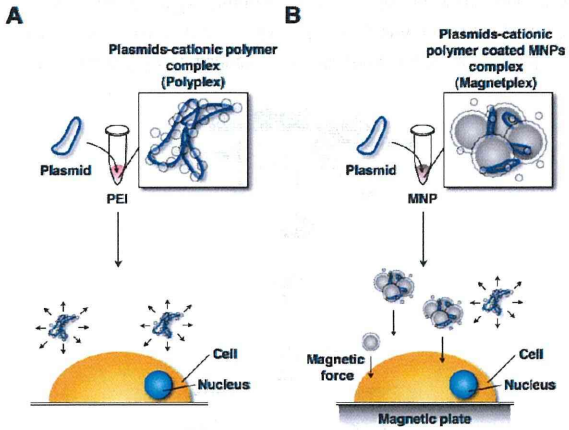

Many researchers have described magnetofection methods (Table 3). They modified the surface of iron oxide-based MNPs to increase transfection efficiency and reduce cytotoxicity. To achieve this, some investigators selected coating agents such as anionic surfactants (oleic acid, lauroyl sarcosinate) [42,50,102], a non-ionic water-soluble surfactant (Pluronic F-127) [42], fluorinated surfactant (lithium 3-[2-(perfluoroalkyl) ethylthio]propionate) [54], a polymer (polyethylene glycol, poly-L-lysine, poly(propyleneimine) dendrimers) [40,103,104], carbohydrates (Chitosan, Heparan sulfate) [41,47], silica particles (MCM48) [49], proteins (serum albumin, streptavidin) [40,55], hydroxyapatite [105], phospholipids [49,50], a cationic cell penetrating peptide (TAT peptide) [43], non-activated virus envelope (HVJ-E) [47], a transfection reagent (Lipofectamine 2000) [53], and viruses (adenovirus, retrovirus) [44,54–56]. These coating agents are often used in conjunction with PEI. PEI is a well-known cationic gene carrier with high transfection efficiency. However, the high toxicity, depended on its molecular weight, has limited its use as a potential gene carrier. Thus, the PEI was modified to increase transfection efficiency, and decrease cytotoxicity [88,106]. To enhance transfection

efficiency, most researchers used the PEI, or the modified PEI to coat the nanoparticle surface [38,41,42,44–46,48,49,51,54,55,102,107]. PEI-coated MNPs are stable in water, bind nucleic acids, and control MNP behavior by magnetic force. In addition, linear PEI possesses low cytotoxicity compared with branched PEI *in vivo* and *in vitro* [108,109] The highest transfection efficiencies have been achieved using 25,000 molecular weight linear PEI [89]. However, PEI cytotoxicity due to its acyl groups has been described [88]. Therefore, our group focused on commercial deacylated PEI (Polyethylenimine "Max" (PEI "Max"), Polysciences Inc.) as an MNP (γ-Fe_2O_3, d = 70 nm, CIK NanoTek) coating agent.

Deacylated polyethylenimine (linear, 25,000 molecular weight) is built from the same polymer backbone as the popular linear polyethylenimine, and possesses high cationic reactivity. PEI "Max"-coated MNPs (PEI max-MNPs) are stable in deionized water, and positively charged. Thus, PEI max-MNPs electrostatically bind to plasmids. We attempted to introduce the green fluorescent protein (GFP) gene into a mouse embryonic carcinoma cell line, P19CL6 using PEI max-MNPs, and succeeded in establishing a highly efficient and low cytotoxic gene delivery system [107]. Furthermore, we applied this system to human fetal lung-derived fibroblasts (TIG-1 cells) using six-well plates. Using MNPs, the transfected gene's expression level increased 2- to 4-fold under optimum conditions (Figure 4, unpublished data). Furthermore, to assess whether the multiple plasmids were expressed in a single cell, we attempt to induce the expression of three fluorescent proteins GFP, cyan fluorescent protein (CFP), and yellow fluorescent protein (YFP). Most cells expressed these three proteins (Figure 5, unpublished data) indicating that gene delivery using MNPs could introduce and allow expression of multiple genes in a single cell.

Figure 4. Optimum conditions for PEI max-MNPs magnetofection. To optimize conditions, we varied volume (**A**) and time on the magnetic plate (**B**). These results were evaluated by quantitative real-time RT-PCR. The relative expression level (*GFP/GAPDH*) in the human fetal lung-derived fibroblasts (TIG-1 cells) treated with PEI max alone (A), and in the absence of magnetic force (0 h) (B) was defined as 1. Optimal transfection conditions were established when TIG-1 cells were treated with 0.8 μg PEI max-MNPs and 2.0 μg pCAG-GFP for 8 h on the magnetic plate in either a six-well plate or a 35 mm dish. The asterisk (*) indicates a significant difference ($P < 0.05$).

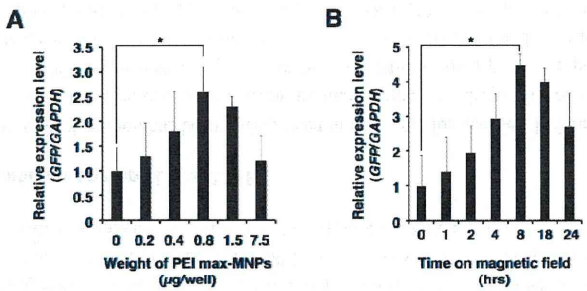

Table 3. Summary of magnetofection literature.

Author	Year	Vector	Magnetic Nanoparticles	Modifying Agent	Targeting Cell, or Tissue	TF Efficiency	Cell Viability (% of Control)	Reference
Kami D	2011	Plasmid	Iron oxide (γ-Fe_2O_3)	PEI max (MW: 25 k)	P19CL6	* 82%	100%	[107]
Pickard MR	2011	Plasmid	NeuroMag	-	Neural procursor cell	* 30%	70%	[39]
Hashimoto M	2011	Adenovirus, Biotin	SPION	PEI, Streptoavidin	HeLa	** 4-fold	-	[55]
		Adenovirus, Biotin	SPION	PEI, Streptoavidin	NIH3T3	** 10-fold	-	
		Adenovirus, Biotin	SPION	PEI, Streptoavidin	Mouse embryonic brain	-	-	
Biswas S	2011	Plasmid	Iron oxide (Fe_3O_4)	Aminooxy, Oxime ether	MCF-7	** 1425-fold	89%	[110]
B González	2011	Plasmid	SPION	Poly(propyleneimine) dendrimers	Saos-2 osteoblasts	* 12%	75%	[104]
Zhang H	2010	Plasmid	SPION	Branch PEI (MW: 25 k)	NIT3T3	* 64%	100%	[38]
		siRNA	SPION	Branch PEI (MW: 25 k)	NIT3T3	* 77%	100%	
Song HP	2010	Plasmid	PolyMag	Tat peptide	U251	* 60%	80%	[43]
		Plasmid	PolyMag	Tat peptide	Rat spinal cord	** 2-fold	-	
Arsianti M	2010	Plasmid	Iron oxide	Branch PEI (MW: 25 k)	BHK-21	-	60–90%	[51]
Shi Y	2010	Plasmid	Magnetite	Hyperbranch PEI (MW: 10 k)	COS-7	** 13-fold	-	[45]
Ang D	2010	Plasmid	Magnetite	Branch PEI (MW: 25 k)	COS-7	** 6-fold	70%	[46]
Tresilwised N	2010	Adenovirus	Iron oxide (Fe_2O_3, Fe_3O_4)	Branch PEI (MW: 25 k), Zonyl FSA fluorosurfactant	EPP85-181RDB	** 10-fold	-	[54]
Namgung R	2010	Plasmid	SPION	PEG, Branch PEI (MW: 25 k)	HUVEC	** 12-fold	80%	[48]
Yiu HH	2010	Plasmid	Iron oxide (Fe_3O_4)	PEI (MW: 25 k), MCM48 (Silica particle)	NCI-H292	** 4-fold	-	[49]
HC Wu	2010	Plasmid	Magnetite	Hydroxyapatite	Rat marrow stromal cells	* 60–70%	100%	[105]
Namiki Y	2009	Plasmid	Magnetite	Oleic acid, Phospholipid	HSC45	** 8-fold	-	[50]
		siRNA	Magnetite	Oleic acid, Phospholipid	Tissue sample from gastric cancer	-	-	
Kim TS	2009	Plasmid	PolyMag	-	Boar spermatozoa	-	-	[52]
Kievit FM	2009	Plasmid	SPION	PEI (MW: 25 k)	C6	* 90%	10%	[41]
		Plasmid	SPION	PEI (MW: 25 k), Chitosan	C6	* 45%	100%	
		Plasmid	PolyMag	-	C6	* 32%	66%	

Table 3. *Cont.*

Author	Year	Vector	Magnetic Nanoparticles	Modifying Agent	Targeting Cell, or Tissue	TF Efficiency	Cell Viability (% of Control)	Reference
Lee JH	2009	siRNA	MnMEIO	Serum albumin, PEG-RGD	MDA-MB-435-GFP	* 30%	-	[40]
Li Z	2009	Plasmid	Iron oxide	Poly-L-lysine	Lung tissue	*** 60%	-	[103]
Yang SY	2008	Plasmid	Iron oxide (Fe_2O_3)	Lipofectamine 2000	He99	-	-	[53]
		Plasmid	Iron oxide (Fe_3O_4)	DOTAP:DOPE	He99	-	-	
Pan X	2008	Plasmid	Magnetite	Oleic acid, Branch PEI (MW: 25 k), Transferrin	KB	** 300-fold	92%	[102]
Mykhaylyk O	2007	Plasmid	Iron oxide (Fe_2O_3, Fe_3O_4)	Branch PEI (MW: 25 k)	H441	* 49%	-	[42]
		Plasmid	Iron oxide (Fe_2O_3, Fe_3O_4)	Pluronic F-127	H441	* 37%	-	
		Plasmid	Iron oxide (Fe_2O_3, Fe_3O_4)	Lauroyl sarcosinate	H441	-	-	
		Plasmid	Iron oxide (Fe_2O_3, Fe_3O_4)	Branch PEI (MW: 25 k), Lauroyl sarcosinate	H441	-	-	
Morishita N	2005	Plasmid	Iron oxide (γFe_2O_3)	HVJ-E, protamine sulfate	BHK-21	** 4-fold	-	[47]
		Plasmid	Iron oxide (γ-Fe_2O_3)	HVJ-E, heparin sulfate	Liver, BALB/c mice (8 weeks age)	** 3-fold	-	
Scherer F	2002	Plasmid	SPION	PEI (MW: 800 k)	NIH3T3	** 5-fold	-	[44]
		Adenovirus	SPION	PEI (MW: 800 k)	K562	** 100-fold	-	
		Retrovirus	SPION	PEI (MW: 800 k)	NIH3T3	* 20%	-	
Mah C	2002	Adenovirus	Avidinylated magnetite	Biotunylated heparan sulfate	C12S	* 75%	-	[56]
		Adenovirus	Avidinylated magnetite	Biotunylated heparan sulfate	Adult 129/SvJ mice	-	-	

* indicates % of fluorescent positive cells analyzed by flow cytometric analysis.

** indicates analysis by luciferase activity assay compared with control. Transfection efficiency was indicated optimal transfection condition.

*** indicates transfection without magnetic force.

PEI: Polyethylenimine; PEI max: Deacylated PEI; MNP: Magnetic nanoparticle; SPION: Superparamagnetic iron oxide nanoparticle; MW: Molecular weight; TF: transfection; PolyMag: Commercial Magnetofection reagent), NeuroMag (Commercial Magnetofection reagent); HVJ-E: hemagglutinating virus of Japan-envelope; DOTAP: 1,2-dioleoyl- 3-trimethylammonium-propane; DOPE: 1,2-dioleoyl-3-sn- phosphatidyl-ethanolamine; Tat peptide: cationic cell penetrating peptide; MeMEIO: Manganese-doped magnetism-engineered iron oxide; PEG: polyethylene glycol, Zonyl FSA fluorosurfactant: Lithium 3-[2-(perfluoroalkyl)ethylthio]propionate).